

Hidden magnetic instability in the substituted multiferroics (Nd, Tb)Fe₃(BO₃)₄I. V. Golosovsky ^{1,*}, A. A. Mukhin ², V. Skumryev ³, E. Ressouche ⁴, V. Yu. Ivanov ² and I. A. Gudim ⁵¹National Research Center “Kurchatov Institute”, B. P. Konstantinov Petersburg Nuclear Physics Institute, 188300 Gatchina, Russia²Prokhorov General Physics Institute, RAS, 119991 Moscow, Russia³Institució Catalana de Recerca i Estudis Avancats, E-08010 Barcelona, Spain⁴Université Grenoble Alpes, CEA, IRIG, MEM, MDN, 38000 Grenoble, France⁵Kirenskii Institute of Physics, Siberian Division of RAS, 660038 Krasnoyarsk, Russia (Received 18 August 2023; revised 26 November 2023; accepted 8 January 2024; published 24 January 2024)

In the substituted Nd_{1-x}Tb_xFe₃(BO₃)₄ ($x = 0.1$ and $x = 0.2$), possessing almost easy-axis magnetic structure at low temperatures, an unusual two-step transition in fields along the trigonal c axis was observed by magnetization and single-crystal neutron diffraction studies. At the first step, only part of the Tb Ising-type moments flip to the c axis, which is accompanied by a significant deviation of the antiferromagnetic Fe spins from the c axis. At the second step, the remaining Tb moments flip and the Fe moments flop into the basal plane. The observed evolution is qualitatively explained by a model assuming small deviations of Tb moments from the trigonal axis due to local environment distortions, which leads to nonequivalence of the Tb ions with respect to effective Tb-Fe exchange and external field. Thus, an intrinsic “hidden” instability of the magnetic system in the magnetic field occurs.

DOI: [10.1103/PhysRevB.109.014421](https://doi.org/10.1103/PhysRevB.109.014421)**I. INTRODUCTION**

Rare-earth ferrobates RFe₃(BO₃)₄, a class of noncentrosymmetric multiferroics with a rhombohedral structure of the huntite mineral, continue to attract considerable attention [1]. The recent interest in these compounds is caused by the strong dependence of the electric polarization on the magnetic field and the giant quadratic magnetoelectric effect, which is important for practical applications [2–7]. Ferrobates demonstrate interesting magnetic properties since they contain strongly interacting rare earth and iron subsystems. This leads to complex magnetic behavior, which is governed by competitions of the magnetocrystalline anisotropy of the iron subsystem and the rare-earth single-ion anisotropy. The rare-earth ions are relatively far apart, their interaction is weak, and the intrinsic spontaneous magnetic order in the rare-earth sublattice does not take place down to very low temperatures. Below the Néel temperature 30–35 K, the iron sublattice with strong isotropic Fe-Fe magnetic exchange interaction, which determines an antiferromagnetic ordering and the Néel temperature, induces the magnetic order in the rare-earth sublattice.

There are two types of antiferromagnetic order in the ferrobates: the “easy-plane” type, as in NdFe₃(BO₃)₄ [8,9], with Fe spins within the basal plane, perpendicular to the trigonal axis, and the “easy-axis” type, as in TbFe₃(BO₃)₄ [10], with spins aligned along the trigonal axis. In the mixed compositions (Nd, Tb)Fe₃(BO₃)₄, the competition between the Fe and R single-ion anisotropies and the R-Fe exchange contribution to the effective magnetic anisotropy leads to a

complex magnetic structure [11]. The zero field temperature evolution for Nd_{1-x}Tb_xFe₃(BO₃)₄ ($x = 0.1$ and $x = 0.2$) was established [11]. At low temperature (~ 2 K) the magnetic structure was found to be close to the easy-axis type with additional fine features.

It is worth mentioning that spontaneous polarization appears in the easy-plane state. In contrast to multiferroics with a centrosymmetric crystal structure, where the electric polarization is determined by an incommensurate cycloidal magnetic order that breaks the inversion symmetry [12,13], the crystal structure in ferrobates is noncentrosymmetric and the electric polarization is induced by an exchange field from the collinear antiferromagnetic Fe subsystem or by the external magnetic field and depends on rare-earth ion type.

This work continues our studies on the magnetic structures in the zero field [11] and the spin-wave dynamics [14] in the substituted system Nd_{1-x}Tb_xFe₃(BO₃)₄, with $x = 0.1$ and $x = 0.2$. Here we present a single-crystal neutron diffraction study of this system in the magnetic field. The present study reveals an unusual two-step field-induced transition from the easy-axis to the basal plane via the angular phase for the Fe moments, which is explained by local anisotropy changes due to structural distortions around the Tb ions.

II. EXPERIMENT

The single-crystal neutron diffraction experiments were carried out at the lifting-counter two-axis diffractometers D15 and D23 [15] at the Institute Laue-Langevin (Grenoble, France) with a constant neutron wavelength of 1.172 and 1.283 Å, respectively. Millimeter-size single crystals with the nominal compositions Nd_{0.9}Tb_{0.1}Fe₃(BO₃)₄ and Nd_{0.8}Tb_{0.2}Fe₃(BO₃)₄ were prepared. The crystals were

*golosovsky-iv@pnpi.nrcki.ru

enriched with the isotope ^{11}B to decrease neutron absorption. For experiments in the magnetic fields the crystals were mounted inside the cryomagnet with a vertical magnetic field, along the c axis of the crystal.

The diffraction patterns were analyzed using the FULLPROF SUITE package [16] in the single-crystal option. Because the isotope ^{11}B has small neutron absorption, no absorption correction was taken into account. However, the single crystals were rather large and had an irregular shape; the refinement of the magnetic structure parameters included correction for anisotropic extinction. The extended model of extinction with three independent parameters was taken into account [16]. The scale factor was refined from the nuclear reflections and fixed in the magnetic refinement.

Bulk magnetic measurements were carried out using a superconducting quantum interference device (SQUID) magnetometer and a physical property measurement system (PPMS) from Quantum Design on the same samples used for neutron diffraction.

III. RESULTS

A. Magnetization

For the two studied compositions, the magnetization in the magnetic field applied along the c axis demonstrates an unusual two-step transition [Figs. 1(a) and 1(b)] instead of the expected one-step transition observed in $\text{TbFe}_3(\text{BO}_3)_4$ [Fig. 1(d)]. The latter is attributed to flop of the Fe spins from the c axis to the basal plane accompanied by magnetization jump associated with a flip of the Tb Ising-type moments from an antiferromagnetic order to a ferromagnetic order [10]. It is plausible to associate the observed magnetization jumps in $(\text{Nd}, \text{Tb})\text{Fe}_3(\text{BO}_3)_4$ with spin flips of Tb moments, which also collaborate with the expected magnetization value at the second step. For the substituted compositions, the magnetization increases linearly after the second transition (see inserts in Fig. 1). We attribute this to the perpendicular susceptibility of the antiferromagnetic aligned Nd moments polarized by Nd-Fe exchange. The contribution from the canting of the antiferromagnetic Fe sublattice is much less because of the strong exchange interaction.

The two-step field-induced transition demonstrates hysteresis. The corresponding critical fields increase with increasing the Tb concentration from $x = 0.1$ to 0.2, with the tendency of closing the field gap in between and, at higher concentrations, of merging the single field-induced transition of $\text{TbFe}_3(\text{BO}_3)_4$. To shed light on the evolution of the magnetic structure at the observed unusual two-step field-induced transition, single-crystal neutron diffraction experiments were performed.

B. Single-crystal neutron diffraction in the magnetic field

The refinement of the neutron diffraction data was based on the antiferromagnetic reflections with the propagation vector $\mathbf{k} = [0\ 0\ 1.5]$ [11]. Note that only antiferromagnetic components of the moments participate in this refinement.

The magnetic moments of Nd and Tb, induced by the exchange field from the Fe sublattice, are opposite, as expected from the different Landé factors of the rare-earth

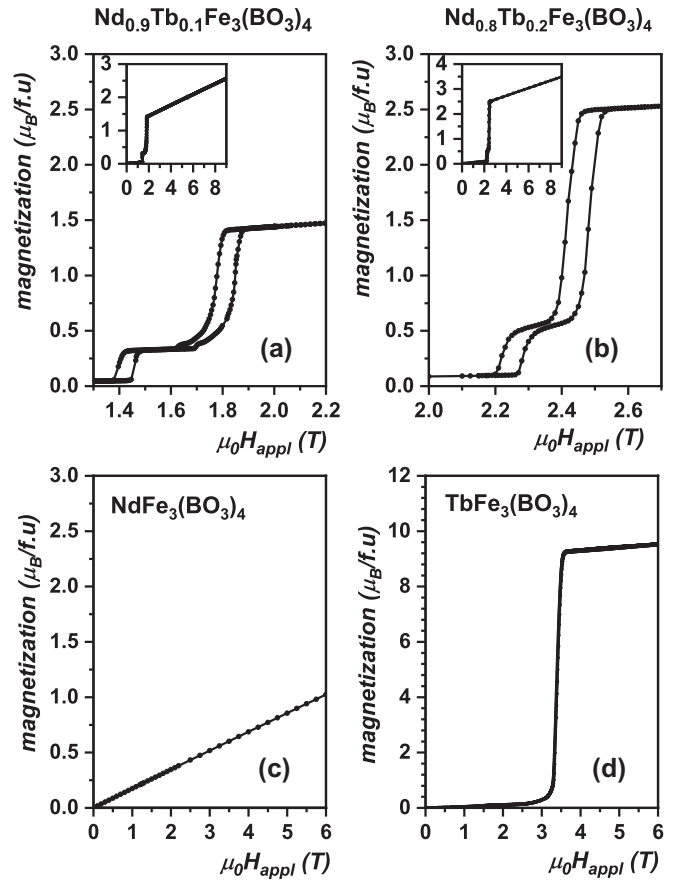


FIG. 1. Dependence of the magnetization in $\text{Nd}_{0.9}\text{Tb}_{0.1}\text{Fe}_3(\text{BO}_3)_4$ (a), $\text{Nd}_{0.8}\text{Tb}_{0.2}\text{Fe}_3(\text{BO}_3)_4$ (b), $\text{NdFe}_3(\text{BO}_3)_4$ (c) and $\text{TbFe}_3(\text{BO}_3)_4$ (d) in the magnetic field applied along the c axis at 2 K. In the inserts the magnetizations in enlarged scale are shown.

ions [11]. Consequently, the contribution to the intensity of the diffraction reflections from the rare-earth sublattice is small in comparison with the Fe spin contribution. Because of this and the small number of the measured reflections, it was impossible to refine all moment magnitudes and their directions simultaneously.

Therefore, following the procedure suggested in Ref. [11] we used the constraints implied by the fact that magnetic order in the rare-earth system of Nd is induced by the Fe sublattice, while Tb is an Ising-type ion. The implemented constraints are based on the parameters of the ground Kramers doublet of Nd^{3+} and the quasidoublet of Tb^{3+} , known for the easy-plane and easy-axis compounds $\text{NdFe}_3(\text{BO}_3)_4$ and $\text{TbFe}_3(\text{BO}_3)_4$, respectively [17–20]. The only difference from the refinement procedure used in Ref. [11] and the present study is that we have taken into account calculation of the external magnetic field.

The exchange field acting on the rare-earth ions from the Fe antiferromagnetic subsystem is staggered (i.e., its sign depends on the rare-earth position), in contrast with the external field. Therefore, there are two different sites for Nd ions: in one site, the exchange field sums with the external field; in the other site, these fields are subtracted. The calculated dependencies of the inclination angle of the Nd^{3+} moment

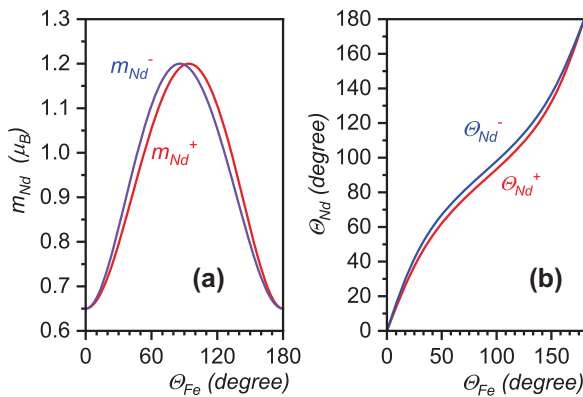


FIG. 2. The calculated dependencies of the inclination angle and the moment of the Nd^{3+} ion versus the inclination angle of the Fe^{3+} spin. The solid lines in the figure correspond to two Nd sites (see text). The calculations in the external field of 1.55 T are shown for the $\text{Nd}_{0.9}\text{Tb}_{0.1}\text{Fe}_3(\text{BO}_3)_4$ compound.

and its magnitude vs the inclination angle of the Fe^{3+} spin for $\text{Nd}_{0.9}\text{Tb}_{0.1}\text{Fe}_3(\text{BO}_3)_4$ in the external magnetic field of 1.55 T are shown in Fig. 2.

In the refinement, we took into account these constraints (Fig. 2) for the inclination angles of the Fe spins and Nd moments and fixed the Tb moments along the c axis. To simplify the calculation, we used the average inclination angle of the Nd^{3+} moment from the c axis and the average moment for two sites following the plots in Fig. 2.

So, a set of variables in the refinement is reduced to the Fe^{3+} magnetic moment and its inclination angle from the c axis. As to the direction of Fe^{3+} spins within the ab plane, the refinement does not show any preferential orientation of these spins, supposedly due to the very small magnetic anisotropy within the basal plane. Therefore, the azimuthal angles were fixed at 90° with respect to the a axis. The trigonal symmetry of the crystal allows the existence of three equivalent domains corresponding to three crystallographic axes in

the ab plane [11]. Therefore, the three-domain approach was considered an adequate model for our refinement.

In the refinement of the neutron diffraction data we assume that, at the first transition, part of the Tb moments undergo the “spin-flip” transition and align ferromagnetically, while the rest of the Tb moments remain in their initial antiferromagnetic arrangement. The relative amounts of “flipped” and “nonflipped” Tb moments were estimated from the magnetization curves (Fig. 1). Thus, the fraction of the “nonflipped” Tb moments, which contribute to antiferromagnetic reflections, was estimated at 78.8% and 84% for $x = 0.1$ and 0.2, respectively, and was fixed in refinement. The Tb moment was taken to be $8.6 \mu_B$ [10].

At the second transition the remaining antiferromagnetic Tb moments also flip. In this way, the refinement procedure is reduced to finding of the Fe subsystem parameters, e.g., the Fe magnetic moment and its orientation with respect to the c axis. The magnetic structures at different magnetic fields at 2 K are shown in Fig. 3. The corresponding parameters are shown in Table I.

The quality of the refinement performed for $\text{Nd}_{0.9}\text{Tb}_{0.1}\text{Fe}_3(\text{BO}_3)_4$ is shown in Fig. 4. The refined magnetic structure in zero field, in the ground state, is close to the easy-axis configuration and is consistent with the structure reported in Ref. [11] refined from 717 reflections.

Because of the Ising character of the Tb^{3+} moment, the role of Tb is to increase in the effective uniaxial anisotropy, which stabilizes the easy-axis antiferromagnetic structure, observed in the zero field. Indeed, before the first transition, in small fields, the magnetic structure is close to the easy-axis configuration (Fig. 3), similar to $\text{TbFe}_3(\text{BO}_3)_4$ [10].

In the intermediate state, there is an “angular” canted configuration. The features of this configuration are (i) the inclination of the Fe spins and coupled Nd moments relative to the c axis and (ii) the coexistence of “flipped” and “nonflipped” Tb moments.

With increasing field, the remaining nonflipped Tb moments in turn undergo a flip from an antiferromagnetic

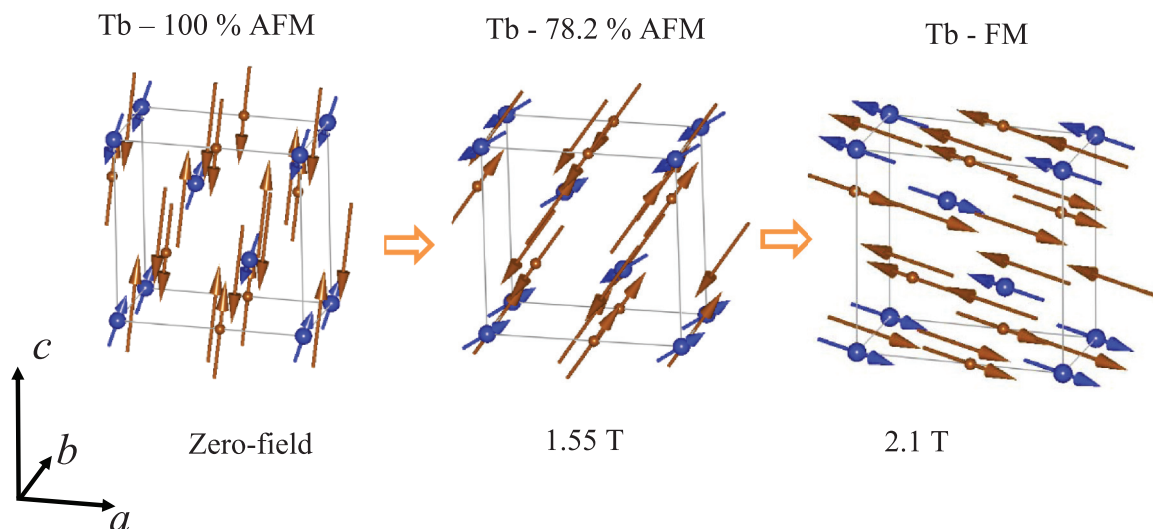


FIG. 3. Evolution of the antiferromagnetic structure of $\text{Nd}_{0.9}\text{Tb}_{0.1}\text{Fe}_3(\text{BO}_3)_4$ in the field. Moments of Fe and Nd are shown in orange and blue, respectively. The moments of Nd are shown enlarged. Antiferromagnetic Tb moments were fixed along the c axis and are not shown.

TABLE I. Refined parameters of the magnetic structures. There are 185 reflections for both compounds. The error (e.s.d.) is shown in parentheses.

	Moment (μ_B)	Inclination angle from the c axis (degrees)	Moment (μ_B)	Inclination angle from the c axis (degrees)
	Nd _{0.9} Tb _{0.1} Fe ₃ (BO ₃) ₄		Nd _{0.8} Tb _{0.2} Fe ₃ (BO ₃) ₄	
		$H = 0$ T		$H = 0$ T
Nd	0.48 fixed	25(4)	0.48 fixed	28(3)
Fe	4.20(2)	10(2)	4.10(1)	12(2)
		$H = 1.55$ T		$H = 2.35$ T
Nd	0.9 fixed	62(2)	0.81 fixed	51(1)
Fe	4.20(3)	41(1)	4.09(1)	34(1)
		$H = 2.1$ T		$H = 4.0$ T
Nd	1.2 fixed	101(3)	1.18 fixed	93(4)
Fe	4.39 fixed	101(3)	4.39(2)	93(4)

arrangement to a ferromagnetic arrangement along the c axis, manifested in the second transition. In this high-field arrangement, the refinement of the neutron diffraction data reveal that the moments of Nd and Fe lie close to the basal plane, perpendicular to the c axis, i.e., perpendicular to the applied magnetic field, and thus the “spin-flop” transition is completed. A small deviation from the ab plane is explained by the error of refinement and poor sample adjustment in the vertical magnetic field.

It should be noted that the proposed model with flipped and nonflipped Tb moments does not suggest any macroscopic

magnetic inhomogeneity. In Fig. 5 two diffraction profiles of the nuclear reflection $0 -3 0$ and the magnetic reflection $0 2 -0.5$ are shown. These reflections have close angles of diffraction, and, hence, they are measured with the same resolution. It is seen that their widths are practically the same. So, there is no magnetic peak broadening, which could indicate formation of magnetic inhomogeneities. This means that the magnetic correlation length coincides with the atomic one; i.e., on the average, a magnetic order is homogeneous throughout the crystal. Moreover, the width of the magnetic peaks does not change with a field or temperature (Fig. 6). The only intensity changes due to transformation of the magnetic structure.

IV. DISCUSSION

We propose that in the studied system (Nd, Tb)Fe₃(BO₃)₄ the observed two-stage field-induced transition results from the difference in the single-ion anisotropy of Tb³⁺ and Nd³⁺ ions and reflexes in intrinsic “hidden” magnetic instability, which manifests itself in the peculiar response to the external magnetic field.

The proposed scenario is based on the assumption that the Ising axes of Tb moments deviate from the c axis by a small angle, of the order of a few degrees. Wherein, the corresponding components in the basal plane are oriented through

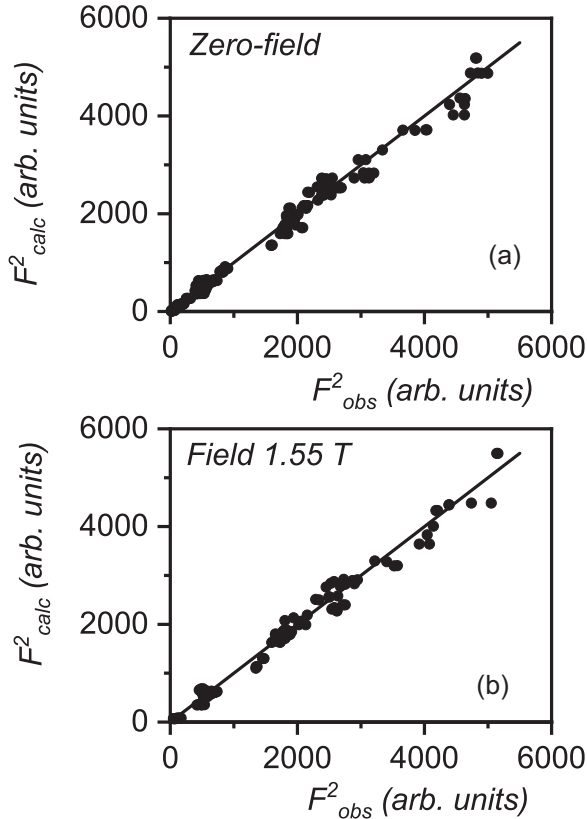


FIG. 4. The results of refinement for Nd_{0.9}Tb_{0.1}Fe₃(BO₃)₄ in zero field, 183 reflections, and R_F factor: 7.5 (a), and in a magnetic field of 1.55 T, 123 reflections, and R_F factor: 6.91 (b).

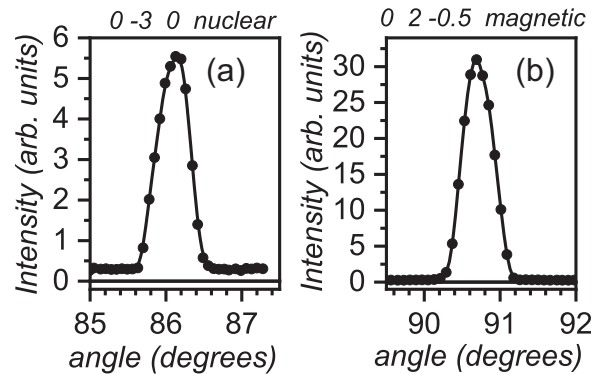


FIG. 5. The rocking curves of the nuclear reflection $0 -3 0$ (a) and the magnetic reflection $0 2 -0.5$ (b) for Nd_{0.9}Tb_{0.1}Fe₃(BO₃)₄, measured at 2 K in a magnetic field of 1.55 T.

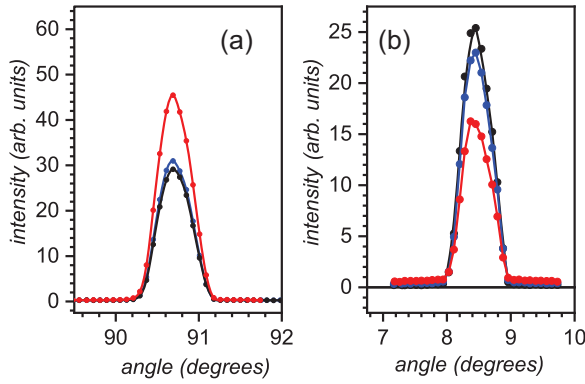


FIG. 6. (a) Temperature dependence of the magnetic reflection 0.0 2.0 -0.5 : at 2 K (in black), at 15 K (in blue), and at 25 K (in red). (b) Field dependence of the magnetic reflection 0.0 2.0 -0.5 : at zero field (in black), at a field of 1.55 T (in blue), and at a field of 2.1 T (in red) $\text{Nd}_{0.9}\text{Tb}_{0.1}\text{Fe}_3(\text{BO}_3)_4$.

120° , which preserves the trigonal symmetry of the crystal on average. This order is shown schematically in Fig. 7(a), where the Tb moments are aligned up and down by the staggered Tb-Fe exchange field.

The deviation of the Tb moments from the c axis results from a local decrease in the symmetry of the environment of the Tb^{3+} ion. Here we suggest its reducing down to C_2 , with the second-order axes in the basal plane at angles of 0 and $\pm 120^\circ$, which corresponds to the space group $P3_121$, realized in pure $\text{TbFe}_3(\text{BO}_3)_4$. Whereas the Nd^{3+} environment keeps local symmetry, D_3 remains more symmetrical and corresponds to the space group $R32$, as in $\text{NdFe}_3(\text{BO}_3)_4$ [8,9].

There is experimental evidence in favor of deviation of the Tb Ising axis from the c axis. Small deviations of Tb moments are difficult to detect using conventional single-crystal neutron diffraction. However, the simulation of the Tb^{3+} optical spectra in $\text{TbFe}_3(\text{BO}_3)_4$ gives small but nonzero projections of the local g factor for the ground quasidoublet of the Tb^{3+} ion which are $g_{yz} = 0.62(1)$ and $g_{zz} = 17.5(3)$ and correspond to the deviation of the Ising axis from the c axis of $\sim 2^\circ$ [21].

Furthermore, in the powder diffraction pattern of $\text{TbFe}_3(\text{BO}_3)_4$, a weak magnetic reflection of $0\ 0\ 1/2$ was observed [10]. In magnetic diffraction only the moment

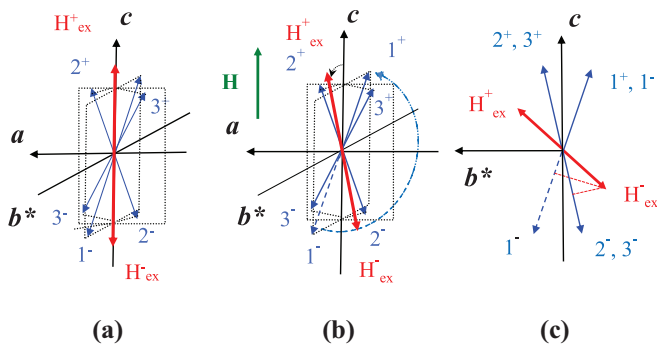


FIG. 7. (a) Tb moments in zero field, oriented along with the staggered exchange field (1^+ , 2^+ , 3^+) and the opposite (1^- , 2^- , 3^-). (b) Tb moments in the external field, in the intermediate state. (c) Projection of Tb moments on the b^*c plane.

projections, which are perpendicular to the diffraction vector, are measured. Because of strong exchange in the Fe subsystem, the magnetic order is practically collinear with spins along the c axis. Therefore, the observed reflection $0\ 0\ 1/2$ can result from the in-plane projection of Tb moments only. The intensity of this reflection corresponds to a magnetic moment of $\sim 0.5 \mu_B$. For the Tb^{3+} moment of $8.6 \mu_B$, the deviation of the Ising axis from the c axis is $\sim 3^\circ$.

Such a scenario may well be realized in the substituted compositions $(\text{Nd}, \text{Tb})\text{Fe}_3(\text{BO}_3)_4$, since Tb^{3+} ions have ionic radii smaller than those of Nd^{3+} ions. The gain in lattice energy due to local distortion around Tb^{3+} ions and a decrease in local symmetry lead to a deviation of the Ising axes from the c axis.

Single-crystal neutron diffraction demonstrates the large deviation of the Fe spins from the c axis in an intermediate magnetic field, after the first transition (see Fig. 3). It leads to the appearance of nonequivalent Tb positions with different resulting effective field projections on Tb Ising axes [Fig. 7(b)].

The resulting effective field is the sum of the staggered Tb-Fe exchange field induced by the Fe spins and the external field. With an increase in the external field, the Tb moments marked in Fig. 7 as 1^- , 2^- , and 3^- tend to line up along the field.

Nonequivalence of Tb moments possessing different effective fields results in different instabilities in the field. For example, for the moment labeled 1^- in Fig. 6, the projection of the exchange field is smaller [Fig. 6(c)] than the projections for the moments labeled 2^- and 3^- . Therefore, the spin-flip transition (the instability) for the moment 1^- occurs earlier than for the moments 2^- and 3^- [Fig. 7(c)]. Note that a similar direction of the Fe spin in-plane projections was proposed in $\text{HoFe}_3(\text{BO}_3)_4$ with the $P3_121$ point group [22].

With a further increase of the field, the remaining Tb moments 2^- and 3^- reorient along the field, while the Fe spins reorient to the basal plane; i.e., they experience a spin-flop. As a result, the process of rearrangement of the magnetic structure has two steps.

This model assumes that the net magnetization after the first transition should amount to $1/3$ from the maximal magnetization. However, the experiment shows 22% and 16% for $\text{Nd}_{0.9}\text{Tb}_{0.1}\text{Fe}_3(\text{BO}_3)_4$ and $\text{Nd}_{0.8}\text{Tb}_{0.2}\text{Fe}_3(\text{BO}_3)_4$, respectively. We would like to note that the magnetic measurements with different samples demonstrate that the critical magnetic fields in all samples practically coincide, while the ratio of the flipped and nonflipped Tb moments in the intermediate state differs for different samples. It means that the used model is the idealized one. Apparently, the ratio of the flipped and nonflipped Tb moments strongly depends on defects and their distribution within a sample.

V. CONCLUSION

Our single-crystal neutron diffraction and magnetization study of the substituted $\text{Nd}_{1-x}\text{Tb}_x\text{Fe}_3(\text{BO}_3)_4$ ferroborites revealed an unusual two-step transition induced by magnetic fields along the trigonal c axis. It manifests itself in two consecutive jumps in the magnetization curves, associated with

the flip to the c axis of only part of the Tb Ising moments at the first step, while the remaining part flips at the second step. At the same time the refinement of the neutron data reveals a deviation of the antiferromagnetic Fe moments from the c axis by an angle of $\sim 30\text{--}40^\circ$ and its subsequent flopping into the basal plane, which accompanies the abovementioned Tb moments' transitions. This complicated evolution of the magnetic structure in magnetic field should be governed by the strong competition of magnetocrystalline anisotropy of the iron subsystem and Nd-Fe exchange and Zeeman energy stabilizing the easy-plane state and Tb-Fe exchange stabilizing the easy-axis state where magnetic single-ion anisotropy of rare earth ions is of a primary importance.

To explain the observed field-induced transformation of the magnetic structure, we suggest the existence of local deviations of the Ising axes of Tb moments from the trigonal axis by a few degrees within azimuthal directions through 120° that preserves the trigonal symmetry of the crystal. The deviations of the Tb moments from the c axis could result from a local reduction in the symmetry of the environment of the Tb^{3+} ion possessing an ionic radius smaller than that of the Nd^{3+}

ion and lower C_2 symmetry as in pure $\text{TbFe}_3(\text{BO}_3)_4$. The existence of a nonequivalence of the Tb ions with respect to the effective Tb-Fe exchange and the external field results in instability (reversal) only in part of the Tb ions at the first step, accompanied by the deviation of Fe moments from the c axis by a finite angle, followed by further flopping into the basal plane. Thus, the observed structure of the two-step transition has an intrinsic character and is caused by hidden instability in the magnetic field of the substituted ferroborates with strongly competing magnetic subsystems. One can envisage similar phenomena in other systems with competing magnetic interactions and local anisotropies.

ACKNOWLEDGMENTS

The authors are grateful to Prof. B. Z. Malkin for fruitful discussions. I.V.G. acknowledges financial support from the Russian Foundation for Basic Research under Grant No. 20-02-00109. A.A.M. and V.Yu.I. acknowledge financial support of the magnetic studies and the developed model from the Russian Science Foundation under Project No. 22-42-05004.

-
- [1] A. Tripathy, K. Gautam, K. Dey, S. R. Sahu, A. Ahad, A. Upadhyay, A. Sagdeo, S. Francoual, P. J. Bereciartua, I. Gudim, J. Strempler, V. G. Sathe, and D. K. Shukla, Structural and magnetic interplay in multiferroic $\text{Ho}_{0.5}\text{Nd}_{0.5}\text{Fe}_3(\text{BO}_3)_4$, *Phys. Rev. B* **107**, 214106 (2023).
- [2] A. M. Kadomtseva, Yu. F. Popov, S. S. Krotov, G. P. Vorob'ev, E. A. Popova, A. K. Zvezdin, and L. N. Bezmaternykh, Investigation of the anomalies of the magnetoelectric and magnetoelastic properties of single crystals of the ferroborate $\text{GdFe}_3(\text{BO}_3)_4$ at phase transitions, *Low Temp. Phys.* **31**, 807 (2005).
- [3] A. M. Kadomtseva, A. K. Zvezdin, A. P. Pyatakov, A. V. Kuvardin, G. P. Vorob'ev, Yu. F. Popov, and L. N. Bezmaternykh, Magnetoelastic interactions in rare-earth ferroborates, *J. Exp. Theor. Phys.* **105**, 116 (2007).
- [4] A. K. Zvezdin, S. S. Krotov, A. M. Kadomtseva, G. P. Vorob'ev, Yu. F. Popov, A. P. Pyatakov, L. N. Bezmaternykh, and E. A. Popova, Magnetoelastic effects in gadolinium iron borate $\text{GdFe}_3(\text{BO}_3)_4$, *JETP Lett.* **81**, 272 (2005).
- [5] A. K. Zvezdin, G. P. Vorob'ev, A. M. Kadomtseva, Yu. F. Popov, P. Pyatakov, L. N. Bezmaternykh, A. V. Kuvardin, and E. A. Popova, Magnetoelastic and magnetoelastic interactions in $\text{NdFe}_3(\text{BO}_3)_4$ multiferroics, *JETP Lett.* **83**, 509 (2006).
- [6] K.-C. Liang, R. P. Chaudhury, B. Lorenz, Y. Y. Sun, L. N. Bezmaternykh, V. L. Temerov, and C. W. Chu, Giant magnetoelectric effect in $\text{HoAl}_3(\text{BO}_3)_4$, *Phys. Rev. B* **83**, 180417(R) (2011).
- [7] F. Yen, B. Lorenz, Y. Y. Sun, C. W. Chu, L. N. Bezmaternykh, and A. N. Vasiliev, Magnetic field effect and dielectric anomalies at the spin reorientation phase transition of $\text{GdFe}_3(\text{BO}_3)_4$, *Phys. Rev. B* **73**, 054435 (2006).
- [8] P. Fischer, V. Pomjakushin, D. Sheptyakov, L. Keller, M. Janoschek, B. Roessli, J. Schefer, G. Petrakovskii, L. Bezmaternykh, V. Temerov, and D. Velikanov, Simultaneous antiferromagnetic Fe^{3+} and Nd^{3+} ordering in $\text{NdFe}_3(\text{BO}_3)_4$, *J. Phys.: Condens. Matter* **18**, 7975 (2006).
- [9] M. Janoschek, P. Fischer, J. Schefer, B. Roessli, V. Pomjakushin, M. Meven, V. Petricek, G. Petrakovskii, and L. Bezmaternykh, Single magnetic chirality in the magnetoelectric $\text{NdFe}_3(\text{BO}_3)_4$, *Phys. Rev. B* **81**, 094429 (2010).
- [10] C. Ritter, A. Balaev, A. Vorotynov, G. Petrakovskii, D. Velikanov, V. Temerov, and I. Gudim, Magnetic structure, magnetic interactions and metamagnetism in terbium iron borate $\text{TbFe}_3(\text{BO}_3)_4$: A neutron diffraction and magnetization study, *J. Phys.: Condens. Matter* **19**, 196227 (2007).
- [11] I. V. Golosovsky, A. I. Vasilev, A. A. Mukhin, E. Ressouche, V. Skumryev, I. Urcelay-Olabarria, I. A. Gudim, and L. N. Bezmaternykh, Complex magnetic order in the (Nd, Tb) $\text{Fe}_3(\text{BO}_3)_4$ multiferroic revealed by single-crystal neutron diffraction, *Phys. Rev. B* **99**, 134439 (2019).
- [12] M. Kenzelmann, A. B. Harris, S. Jonas, C. Broholm, J. Schefer, S. B. Kim, C. L. Zhang, S.-W. Cheong, O. P. Vajk, and J. W. Lynn, Magnetic inversion symmetry breaking and ferroelectricity in TbMnO_3 , *Phys. Rev. Lett.* **95**, 087206 (2005).
- [13] T. Goto, T. Kimura, G. Lawes, A. P. Ramirez, and Y. Tokura, Ferroelectricity and giant magnetocapacitance in perovskite rare-earth manganites, *Phys. Rev. Lett.* **92**, 257201 (2004).
- [14] I. V. Golosovsky, A. A. Mukhin, V. Skumryev, M. Boehm, W. Schmidt, L.-P. Regnault, and I. A. Gudim, Magnetic excitations and exchange interactions in the substituted multiferroics (Nd, Tb) $\text{Fe}_3(\text{BO}_3)_4$ revealed by inelastic neutron scattering, *Phys. Rev. B* **103**, 214412 (2021).
- [15] D23 thermal neutron lifting-counter two-axis diffractometer, <https://www.ill.eu/users/instruments/instruments-list/d23/description/instrument-layout>.
- [16] J. Rodríguez-Carvajal, Recent advances in magnetic structure determination by neutron powder diffraction, *Physica B: Condens. Matter* **192**, 55 (1993).

- [17] M. N. Popova, E. P. Chukalina, T. N. Stanislavchuk, B. Z. Malkin, A. R. Zakirov, E. Antic-Fidancev, E. A. Popova, L. N. Bezmaternykh, and V. L. Temerov, Optical spectra, crystal-field parameters, and magnetic susceptibility of multiferroic $\text{NdFe}_3(\text{BO}_3)_4$, *Phys. Rev. B* **75**, 224435 (2007).
- [18] E. A. Popova, D. V. Volkov, A. N. Vasiliev, A. A. Demidov, N. P. Kolmakova, I. A. Gudim, L. N. Bezmaternykh, N. Tristan, Yu. Skourski, B. Buchner, C. Hess, and R. Klingeler, Magnetization and specific heat of $\text{TbFe}_3(\text{BO}_3)_4$: Experiment and crystal-field calculations, *Phys. Rev. B* **75**, 224413 (2007).
- [19] A. K. Zvezdin, A. M. Kadomtseva, Yu. F. Popov, G. P. Vorob'ev, A. P. Pyatakov, V. Y. Ivanov, A. M. Kuz'menko, A. A. Mukhin, L. N. Bezmaternykh, and I. A. Gudim, Magnetic anisotropy and magnetoelectric properties of $\text{Tb}_{1-x}\text{Er}_x\text{Fe}_3(\text{BO}_3)_4$ ferroborates, *J. Exp. Theor. Phys.* **109**, 68 (2009).
- [20] A. M. Kuz'menko, A. A. Mukhin, V. Y. Ivanov, A. M. Kadomtseva, and L. N. Bezmaternykh, Effects of the interaction between R and Fe modes of the magnetic resonance in $\text{RFe}_3(\text{BO}_3)_4$ rare-earth iron borates, *JETP Lett.* **94**, 294 (2011).
- [21] M. N. Popova, T. N. Stanislavchuk, B. Z. Malkin, and L. N. Bezmaternykh, Phase transitions and crystal-field and exchange interactions in $\text{TbFe}_3(\text{BO}_3)_4$ as seen via optical spectroscopy, *J. Phys.: Condens. Matter* **24**, 196002 (2012).
- [22] M. N. Popova, E. P. Chukalina, D. A. Erofeev, I. A. Gudim, I. V. Golosovsky, A. Gukasov, A. A. Mukhin, and B. Z. Malkin, High-resolution optical spectroscopy, magnetic properties, and single-crystal neutron diffraction of multiferroic $\text{HoFe}_3(\text{BO}_3)_4$: Magnetic structure, *Phys. Rev. B* **103**, 094411 (2021).